ESR and ENDOR Investigations of Spin Exchange in Mixed Galvinoxyl/Nitroxide Biradicals. Syntheses

B. Kirste, A. Krüger, and H. Kurreck*

Contribution from the Institut für Organische Chemie, Freie Universität Berlin, 1000 Berlin 33, West Germany. *Received October 13, 1981*

Abstract: The synthesis of a variety of mixed biradicals consisting of galvinoxyl and nitroxide moieties is given. For the first time successful fluid solution ENDOR experiments on mixed biradicals could be performed. The magnetic properties of these systems are significantly dependent (a) on the relative magnitudes of the exchange integral J as compared to the hyperfine interactions, (b) on the sign of J, and (c) on the difference of the g values of the constituent monoradical fragments. It is demonstrated that the ENDOR technique allows direct determination of the hyperfine coupling constants even in cases where $|J|$ is comparable in magnitude to the hyperfine coupling constants. Moreover, the sign of the exchange integral can be deduced from these measurements. It is shown that ENDOR spectroscopy in combination with spin labeling to obtain "weakly coupled biradicals" may serve as a technique to measure signs of hyperfine coupling constants.

In recent years ESR studies have been performed on a large number of different types of organic biradicals, namely, bis(nitroxides),[1] bis(verdazyls),[2] bis(hydrazyls),[3] bis(phenoxyls),[4] bis(galvinoxyls),[5] bis(triphenylmethyls),[6] bis(cyclopentadienyls),[7] and bis(ketyls).[8] Characteristic magnetic properties of these systems are the (anisotropic) electron–electron dipolar interaction, giving rise to the zero-field splitting, and the (scalar) exchange interaction, measured by the exchange integral J. The appearance of the fluid solution ESR spectra depends on the magnitudes of the zero-field splitting parameters D and E and on the relative magnitude of J as compared to the hyperfine coupling constants a. If D is smaller than roughly 100 MHz, this anisotropic interaction is averaged out by the Brownian motion and well-resolved ESR hyperfine spectra can, in principle, be observed. In the limiting case $|J| \ll |a|$, simply a superposition of the spectra of the monoradical halves is obtained, whereas in the case $|J| \gg |a|$, a spectrum characteristic of the hyperfine interaction of each unpaired electron with all magnetic nuclei in the molecule is found. In these latter systems the unpaired electrons can be assumed to be delocalized over the whole molecule rather than confined, each on one monoradical moiety. If the exchange interaction becomes comparable in magnitude to the hyperfine interaction ($|J| \simeq |a|$), rather complex ESR spectra are observed.[9] Yet these spectra are still essentially symmetric (neglecting m_I-dependent line width contributions from anisotropic hyperfine interactions).

The situation becomes even more puzzling if one is dealing with so-called "mixed biradicals", i.e., biradicals consisting of different (mono) radical moieties connected by bridges of different lengths. In this case the g value as well as the hyperfine couplings of the constituent radical fragments will be different. It should be mentioned that a similar problem arising in spin-label studies of metal complexes has been investigated thoroughly.[10]

In the present paper we report on an extensive study of the exchange interaction in mixed galvinoxyl/nitroxide biradicals. We have chosen these systems because the respective galvinoxyl and nitroxide doublet radicals are known to be fairly stable, and they do not dimerize. As a prerequisite a series of novel biradicals had to be synthesized. Since we are currently applying ENDOR spectroscopy in studies of organic paramagnetic molecules, we were particularly interested in exploring whether more detailed information about the hyperfine interaction might be obtained with the ENDOR technique, which is known to yield a higher resolution as compared to conventional ESR. Whereas several papers dealing with ENDOR investigations of triplet-state biradicals have been published, hitherto no ENDOR studies exist of biradicals with $|J| \simeq |a|$. It should be noted that biradicals with $|J| \gg |a|$ show well-defined singlet and triplet states and the ESR transitions $|-1,M_I\rangle \leftrightarrow |0,M_I\rangle$ and $|0,M_I\rangle \leftrightarrow |1,M_I\rangle$ within the triplet manifold are degenerate in isotropic fluid solution. In the intermediate case $|J| \simeq |a|$, the hyperfine interaction results in a mixing of the $M_S = 0$ triplet sublevel with the singlet level. As a consequence, the degeneracy of the transitions $|-1,M_I\rangle \leftrightarrow |0,M_I\rangle$ and $|0,M_I\rangle \leftrightarrow |1,M_I\rangle$ is lifted. In a way this is analogous to the lifting of the degeneracy of the ESR transitions by the zero-field splitting in rigid matrices.[11] The potentiality of selecting one of the ESR transitions might have two consequences. First, ENDOR lines at the free nuclear frequencies might show up. These lines have been predicted theoretically,[12] but they cannot be observed in isotropic fluid solution since both ESR transitions are pumped equally strongly.[13] However, they were recently detected in rigid solutions.[14] Second, it should be possible to determine the signs of the hyperfine splittings relative to that of the exchange integral J. Thus, the sign of J might be determined absolutely, provided the absolute sign of one of the hyperfine couplings is known. This possibility would be of substantial value since J values of the order of magnitude of hyperfine coupling constants are too small to be deducible from susceptibility measurements. The sign of J is normally not accessible from ESR experiments, though in favorable cases it can be derived from liquid crystal measurements[15] or from line width analyses.[16]

To date we have only come across one ESR report, by Kreilick,[17] on a mixed biradical. This mixed phenoxy/nitroxide biradical

(1) Aurich, H. G.; Weiss, W. *Top. Curr. Chem.* **1975**, *59*, 65. Parmon, V. N.; Kokorin, A. I.; Zamaraev, K. I. *Izv. Akad. Nauk SSSR Ser. Khim.* **1976**, 1776.
(2) Neugebauer, F. A.; Bernhardt, R.; Fischer, H. *Chem. Ber.* **1977**, *110*, 2254.
(3) Stashkov, L. I.; Matevosyan, R. O. *J. Org. Chem. USSR (Engl. Transl.)* **1965**, *1*, 624.
(4) Müller, E.; Mayer, R.; Scheffler, K. *Z. Naturforsch. B:* **1958**, *13*, 825.
(5) Gierke, W.; Harrer, W.; Kirste, B.; Kurreck, H.; Reusch, J. *Z. Naturforsch. B: Anorg. Chem., Org. Chem.* **1976**, *31*, 965. Broser, W.; Kirste, B.; Kurreck, H.; Reusch, J.; Plato, M. *Ibid.* **1976**, *31*, 974.
(6) Popp, F.; Bickelhaupt, E.; MacLean, C. *Chem. Phys. Lett.* **1978**, *55*, 327. Broser, W.; Kurreck, H.; Niemeier, W. *Tetrahedron* **1975**, *31*, 1769.
(7) Broser, W.; Janzen, D.; Kurreck, H.; Braasch, D.; Oestreich, S.; Plato, M. *Tetrahedron* **1976**, *32*, 1819.
(8) Oestreich, S.; Kurreck, H. *Tetrahedron* **1974**, *30*, 3199.
(9) Brière, R.; Dupeyre, R. M.; Lemaire, H.; Morat, C.; Rassat, A.; Rey, P. *Bull. Soc. Chim. Fr.* **1965**, 3290.
(10) DuBois, D. L.; Eaton, G. R.; Eaton, S. S. *J. Am. Chem. Soc.* **1979**, *101*, 2624 and references therein. Eaton, S. S.; Eaton, G. R. *Coord. Chem. Rev.* **1978**, *26*, 207.
(11) Wasserman, E.; Snyder, L. C.; Yager, W. A. *J. Chem. Phys.* **1964**, *41*, 1763.
(12) Brauer, H.-D.; Stieger, H.; Hyde, J. S.; Kispert, L. D.; Luckhurst, G. R. *Mol. Phys.* **1969**, *17*, 457.
(13) van Willigen, H.; Plato, M.; Möbius, K.; Dinse, K.-P.; Kurreck, H.; Reusch, J. *Mol. Phys.* **1975**, *30*, 1359.
(14) Kirste, B.; van Willigen, H.; Kurreck, H.; Möbius, K.; Plato, M.; Biehl, R. *J. Am. Chem. Soc.* **1978**, *100*, 7505.
(15) Glarum, S. H.; Marshall, J. H. *J. Chem. Phys.* **1967**, *47*, 1374. Lemaire, H. *J. Chim. Phys. Phys.-Chim. Biol.* **1967**, *64*, 559.
(16) Luckhurst, G. R.; Pedulli, G. F. *Mol. Phys.* **1971**, *20*, 1043.
(17) Kreilick, R. W. *Chem. Phys. Lett.* **1968**, *2*, 277.

0002-7863/82/1504-3850$01.25/0

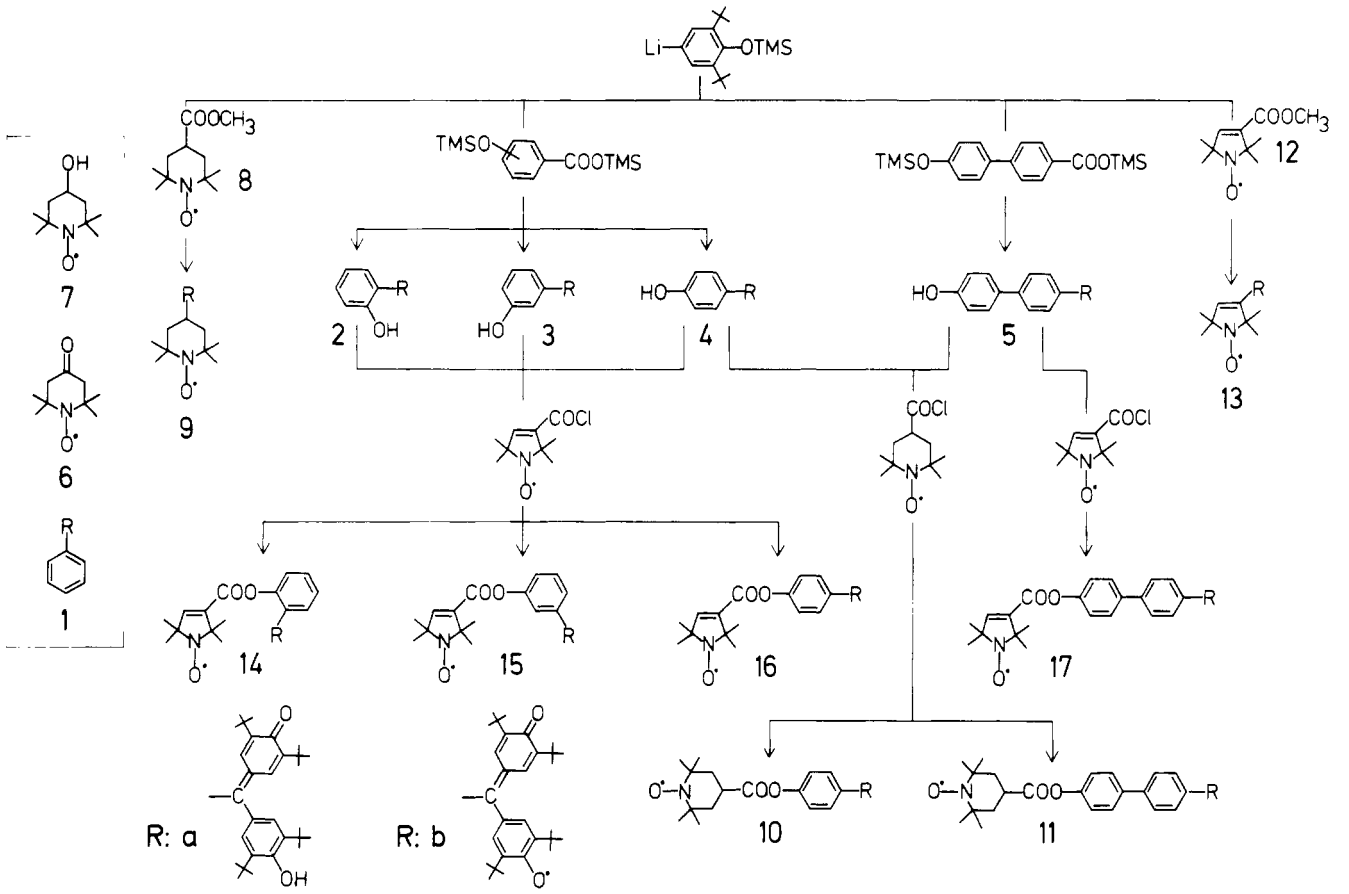

Figure 1. Reaction scheme for the preparation of the mixed galvinoxyl/nitroxide biradicals (TMS = trimethylsilyl). Note the numbering of compounds; **a** and **b** refer to R substituted as either the galvinol or the galvinoxyl moiety (lower left).

Table I. Melting Points, Yields, and Analytical Data of the Galvinols[a]

compound	mp, °C	yield, %	formula (*M*)	microanalysis, % calcd C	calcd H	calcd N	found C	found H	found N
2a, 2-R-phenol	224–225	21	$C_{35}H_{46}O_3$ (514.3)	81.66	9.01		81.92	9.27	
3a, 3-R-phenol	282–283	28	$C_{35}H_{46}O_3$ (514.3)	81.66	9.01		81.46	9.16	
4a, 4-R-phenol	277–278	41	$C_{35}H_{46}O_3$ (514.3)	81.66	9.01		81.58	8.99	
5a, 4-R-4′-hydroxybiphenyl	260–261	27	$C_{41}H_{50}O_3$ (590.4)	83.34	8.54		83.62	8.87	
9a, 4-R-2,2,6,6-tetramethylpiperidin-1-yloxy	211–212	14	$C_{38}H_{58}NO_3$ (576.4)	79.11	10.14	2.43	78.85	10.11	2.39
10a, 1-R-4-[(2,2,6,6-tetramethylpiperidin-1-yloxy-4-yl)(carbonyloxy)] benzene	215–216	23	$C_{45}H_{62}NO_5$ (696.5)	77.54	8.97	2.01	77.71	9.25	1.98
11a, 4-R-4′-[(2,2,6,6-tetramethylpiperidin-1-yloxy-4-yl)(carbonyloxy)] biphenyl	270–271	12	$C_{51}H_{66}NO_5$ (772.5)	79.22	8.61	1.82	79.32	8.56	1.85
13a, 3-R-2,5-dihydro-2,2,5,5-tetramethylpyrrol-1-yloxy	208–209	19	$C_{37}H_{54}NO_5$ (560.4)	79.23	9.71	2.50	79.29	9.74	2.29
14a, 1-R-2-[(2,5-dihydro-2,2,5,5-tetramethylpyrrol-1-yloxy-3-yl)(carbonyloxy)] benzene	254–255	10	$C_{44}H_{58}NO_5$ (680.4)	77.60	8.59	2.06	77.29	8.60	1.77
15a, 1-R-3-[(2,5-dihydro-2,2,5,5-tetramethylpyrrol-1-yloxy-3-yl)(carbonyloxy)] benzene	212–213	17	$C_{44}H_{58}NO_5$ (680.4)	77.60	8.59	2.06	77.51	8.71	1.91
16a, 1-R-4-[(2,5-dihydro-2,2,5,5-tetramethylpyrrol-1-yloxy-3-yl)(carbonyloxy)] benzene	213–214	25	$C_{44}H_{58}NO_5$ (680.4)	77.60	8.59	2.06	77.71	8.73	1.71
17a, 4-R-4′-[(2,5-dihydro-2,2,5,5-tetramethylpyrrol-1-yloxy-3-yl)(carbonyloxy)] biphenyl	256–258	26	$C_{50}H_{62}NO_5$ (756.5)	79.32	8.26	1.85	79.15	8.35	1.81

[a] R = [(3,5-Di-*tert*-butyl-4-hydroxyphenyl)(3,5-di-*tert*-butyl-4-oxocyclohexa-2,5-dienylidene)methyl].

showed an exchange interaction much larger than the hyperfine interaction ($|J| \gg |a|$), but the study was complicated by a dimerization equilibrium of the phenoxy moiety and, to our understanding, the presence of monoradical impurities.

Experimental Section

Preparation of Compounds. The synthesis of mixed biradicals is, in principle, complicated because the two moieties consist of different functional groups, thus calling for different synthetic pathways and exhibiting different chemical properties, (see Figure 1). The most promising route to obtain the esters **10a**, **11a**, and **14a–17a** was first to synthesize both the fragments, i.e., the respectively modified nitroxide and the galvinol. Subsequently, these moieties were connected by esterification. 3-(Chlorocarbonyl)-2,5-dihydro-2,2,5,5-tetramethylpyrrol-1-yloxy[18] (for compounds **14a–17a**) and 4-(chlorocarbonyl)-2,2,6,6-tetramethylpiperidin-1-yloxy[19] (for **10a** and **11a**) were obtained by reaction of the respective carboxylic acids with thionyl chloride. The substituted galvinols were prepared by following our organometallic synthesis de-

(18) Krinitskaya, L. A.; Buchachenko, A. L.; Rozantsev, E. G. *Zh. Org. Khim.* **1966**, *2*, 1301.
(19) Rozantsev, E. G.; Krinitskaya, L. A. *Tetrahedron* **1965**, *21*, 491.

scribed elsewhere.[20] For this purpose the respective benzoic acids[21] were treated with twice the molar amount of chlorotrimethylsilane. The resulting trimethylsilyl esters, protected at the hydroxyl groups with trimethylsilyl, were allowed to react with (2,6-di-*tert*-butyl-4-lithiophenoxy)trimethylsilane. Subsequent elimination of all trimethylsilyl groups yielded the corresponding (hydroxyphenyl)galvinols. Linking of the nitroxide acid chlorides with the (hydroxyphenyl)galvinols was achieved by using absolute pyridine as base. The directly connected nitroxide/galvinol compounds **9a** and **13a** were obtained analogously by the organometallic reaction of the respective methyl esters **8** and **12**.[22] In Table I melting points, yields, and analytical data are collected for all compounds synthesized.

(Hydroxyphenyl)galvinols (2a–5a). The corresponding benzoic acid (10 mmol), suspended in absolute toluene, was treated with chlorotrimethylsilane (22 mmol) and triethylamine (24 mmol) to give trimethylsilyl-protected trimethylsilyl ester. This toluene solution at 0 °C was added to a mixture of (2,6-di-*tert*-butyl-4-bromophenoxy)trimethylsilane (22.5 mmol), *n*-butyllithium (27 mmol) in *n*-hexane (20%), and 4.0 mL of 1,2-bis(dimethylamino)ethane. Hydrolysis and subsequent elimination of the trimethylsilyl group with HCl/CH_3OH (5%) yielded the (hydroxyphenyl)galvinols. The crude materials were recrystallized from toluene.

Nitroxide/Galvinol Esters (10a, 11a, and 14a–17a). A sample, (13 mmol) of 3-carboxy-2,5-dihydro-2,2,5,5-tetramethylpyrrol-1-yloxy or 4-carboxy-2,2,6,6-tetramethylpiperidin-1-yloxy, was converted into the acyl chloride by reaction with thionyl chloride (17 mmol) and pyridine. The solution of the acyl chlorides at 0 °C was added to a pyridine solution of the (hydroxyphenyl)galvinol (10 mmol). The reaction mixture was stirred at room temperature for 2 h and then poured on ice. After extraction with chloroform, purification was achieved by column chromatography on silica gel, with chloroform as eluant.

3-[(3,5-Di-*tert*-butyl-4-hydroxyphenyl)(3,5-di-*tert*-butyl-4-oxocyclohexa-2,5-dienylidene)methyl]-2,5-dihydro-2,2,5,5-tetramethylpyrrol-1-yloxy (13a) and 4-[(3,5-Di-*tert*-butyl-4-hydroxyphenyl)(3,5-di-*tert*-butyl-4-oxocyclohexa-2,5-dienylidene)methyl]-2,2,6,6-tetramethylpiperidin-1-yloxy (9a). A solution (13.5 mmol) of 3-(methoxycarbonyl)-2,5-dihydro-2,2,5,5-tetramethylpyrrol-1-yloxy or 4-(methoxycarbonyl)-2,2,6,6-tetramethylpiperidin-1-yloxy was added to the lithium organic reagent prepared from (2,6-di-*tert*-butyl-4-bromophenoxy)trimethylsilane (30 mmol), *n*-butyllithium (36 mmol) in *n*-hexane (20%), and 5.0 mL of 1,2-bis(dimethylamino)ethane. Subsequent hydrolysis followed by elimination of the trimethylsilyl groups with HCl/CH_3OH (5%) yielded the crude compound, which was purified by column chromatography on silica gel, with chloroform as eluant.

Preparation of Samples. The nitroxide monoradical samples were obtained by dissolving the respective compound in toluene. The biradicals were generated by reaction with PbO_2 or $K_3[Fe(CN)_6]/KOH$ in toluene. The solutions of the radicals were carefully degassed on a high-vacuum line.

Instrumentation. ESR spectra were recorded on a Bruker ER200D ESR spectrometer. The ENDOR and TRIPLE instrumentation basically consists of a Bruker ER220D ESR spectrometer equipped with a Bruker cavity (ER200ENB) and home-built NMR facilities described elsewhere.[23] ENDOR spectra were accumulated by using a Nicolet signal averager 1170 employing 1K data points; typically, 32 sweeps were taken, 30 s per scan. The temperature was varied with a Bruker B-VT1000 temperature control unit, constant to ±1 K and checked by means of a thermocouple. Field and frequency measurements for the *g*-value determinations were performed by using an AEG NMR gaussmeter and a HP5340A frequency counter, respectively. The field gradient was measured and corrected for by comparison with a sample of triphenylmethyl in toluene ($g = 2.002\,588$).[24] Reported *g* values are corrected for second-order contributions.

Theory

When the spin Hamiltonian given by Reitz and Weissman for a *symmetrical* biradical[25] is extended, the appropriate spin Hamiltonian for an *unsymmetrical* biradical in isotropic fluid solution is given by[26]

$$\mathcal{H} = g^{(a)}\beta BS_z^{(a)} - \beta_n \sum_i g_n^{(i)} BI^{(i)} + h \sum_i a_i^{(a)} S^{(a)} I^{(i)} + g^{(b)}\beta BS_z^{(b)} - \beta_n \sum_j g_n^{(j)} BI^{(j)} + h \sum_j a_j^{(b)} S^{(b)} I^{(j)} + hJS^{(a)}S^{(b)} \quad (1)$$

where the labels (a) and (b) refer to the two fragments and not to individual electrons. It should be noted that the spin Hamiltonian (1) is only valid under the condition that the overlap of the molecular orbitals $|a\rangle$ and $|b\rangle$ containing the unpaired electrons can be neglected. It will become evident from the following that only in the limit $|J| \ll |a|$ do the "doublet" hyperfine coupling constants $a_i^{(a)}$ and $a_j^{(b)}$ have a direct experimental meaning; i.e., they are given by the distances of the respective ESR hyperfine components. On the other hand, in the limit, $|J| \gg |a|, |\Delta g\beta B/h|$, the line separation, is given by "triplet" hyperfine coupling constants a_i^t and the spin Hamiltonian can be formulated as[27]

$$\mathcal{H} = g\beta BS_z - \beta_n \sum_k g_n^{(k)} BI^{(k)} + h \sum_k a_k^t SI^{(k)} + \tfrac{1}{2}hJ(S^2 - \tfrac{3}{2}) \quad (2)$$

where $S = S^{(a)} + S^{(b)}$ is the total electron spin operator, $g = (g^{(a)} + g^{(b)})/2$, and $a_i^t = a_i^{(a)}/2$, $a_j^t = a_j^{(b)}/2$ under the above-mentioned condition of negligible overlap between the spatial wave functions; the summation index k refers to all magnetic nuclei present in the biradical.

Before the general case is considered in detail, a brief summary of the simpler situation shall be given, where hyperfine interaction is absent and only the difference in *g* values, $\Delta g = g^{(a)} - g^{(b)}$, has to be taken into account. An excellent description of this system is provided by Luckhurst.[26] It turns out that the respective scalar spin Hamiltonian is formally equivalent to that of an AB system in NMR spectroscopy.[28] The triplet ($|1\rangle, |0_a\rangle, |-1\rangle$) and singlet ($|0_e\rangle$) spin functions may be chosen as a basis set. Whereas the triplet spin functions $|1\rangle$ and $|-1\rangle$ are eigenfunctions of the spin Hamiltonian irrespective of the value of J, the states $|0_a\rangle$ and $|0_e\rangle$ are mixed by the *g*-factor difference. Diagonalization of the Hamiltonian matrix yields the following eigenvalues.[26]

$$\begin{aligned} E_1/h &= \epsilon + \tfrac{1}{4}J \\ E_{0+}/h &= \tfrac{1}{4}J + \tfrac{1}{2}\delta \tan\phi \\ E_{-1}/h &= -\epsilon + \tfrac{1}{4}J \\ E_{0-}/h &= -\tfrac{3}{4}J - \tfrac{1}{2}\delta \tan\phi \end{aligned} \quad (3)$$

where

$$\epsilon = \tfrac{1}{2}\beta B(g^{(a)} + g^{(b)})/h \quad (4)$$

$$\delta = \Delta g\beta B/h \quad (5)$$

$$\tan 2\phi = \delta/J \quad (6)$$

and the eigenfunctions

$$\begin{aligned} |0+\rangle &= (\cos\phi)|0_a\rangle + (\sin\phi)|0_e\rangle \\ |0-\rangle &= (\cos\phi)|0_e\rangle - (\sin\phi)|0_a\rangle \end{aligned} \quad (7)$$

The allowed ESR transitions and relative intensities, *p*, are given by

$$\begin{aligned} \nu(|0-\rangle \leftrightarrow |1\rangle) &= \epsilon + \tfrac{1}{2}\delta \tan\phi + J \\ p &= \sin^2\phi \\ \nu(|-1\rangle \leftrightarrow |0+\rangle) &= \epsilon + \tfrac{1}{2}\delta \tan\phi \\ p &= \cos^2\phi \\ \nu(|0+\rangle \leftrightarrow |1\rangle) &= \epsilon - \tfrac{1}{2}\delta \tan\phi \\ p &= \cos^2\phi \\ \nu(|1-\rangle \leftrightarrow |0-\rangle) &= \epsilon - \tfrac{1}{2}\delta \tan\phi - J \\ p &= \sin^2\phi \end{aligned} \quad (8)$$

(20) Harrer, W.; Kurreck, H.; Reusch, J.; Gierke, W. *Tetrahedron* **1975**, *31*, 625.
(21) Gray, G. W.; Harrley, J. B.; Jones, B. *J. Chem. Soc.* **1955**, 1412.
(22) Rauckman, E. J.; Rosen, G. M.; Abou-Donia, M. B. *J. Org. Chem.* **1976**, *41*, 564.
(23) Fey, H. J.; Kurreck, H.; Lubitz, W. *Tetrahedron* **1979**, *35*, 905.
(24) Segal, B. G.; Kaplan, M.; Fraenkel, G. K. *J. Chem. Phys.* **1965**, *43*, 4191.
(25) Reitz, D. C.; Weissman, S. I. *J. Chem. Phys.* **1960**, *33*, 700.
(26) Luckhurst, G. R. In "Spin Labeling"; Berliner, L. J., Ed.; Academic Press: New York, 1976; p 133.
(27) Kirste, B.; Kurreck, H.; Lubitz, W.; Schubert, K. *J. Am. Chem. Soc.* **1978**, *100*, 2292.
(28) Carrington, A.; McLachlan, A. D. "Introduction to Magnetic Resonance"; Harper and Row: New York, 1967; p 44.

Table II. g Values and Hyperfine Coupling Constants (MHz)[a] of Monoradicals

radical	g[b]	a^{H}_{m}(phenoxy)	$a^{H}_{t\text{-Bu}}$	a^{H}_{o}	a^{H}_{m}	a^{H}_{p}	T, K[c]
1b	2.00463	+3.71 (2 H), +3.56 (2 H)	+0.12	+0.56	−0.22	+0.64	195
radical	g	$a^{H}_{CH_3}$	a^{H}_{3} or a^{H}_{4}	T,[c] K	a^{N}	T, K[d]	
6	2.00610	(−)0.30 (12 H)		195	(+)40.47	225	
7	2.00621	−1.30 (6 H)	−1.60 (2 H), −0.85 (2 H)	185	+43.87	205	
					+43.45	288	
8	2.00623	−1.31 (6 H)	−1.60 (2 H), −0.86 (2 H)	185	+43.87	225	
11a	2.00621	−1.30 (6 H)	−1.54 (2 H), −0.81 (2 H)	225	+43.65	267	
12	2.00591	−0.66 (12 H)	−1.46 (1 H)	185	+39.60	205	
					+39.84	267	
16a	2.00592	−0.67 (12 H)	−1.38 (1 H)	225	+39.83	288	

[a] All HFSC's are measured by ENDOR (toluene), accurate within ±0.01 MHz. 1 MHz ≙ 0.03562 mT (g = 2.006). [b] g values measured at 290 K, accurate within $\pm 1 \times 10^{-5}$. [c,d] Temperature for ^{1}H and ^{14}N ENDOR, respectively. The different temperatures reflect the different optimum ENDOR conditions.

Thus two pairs of ESR lines symmetrically spaced around the mean resonance field ($g = {}^1/_2(g^{(a)} + g^{(b)})$ should be observable, with the inner pair being more intense. The separation of the inner pair, expressed in frequency units, is given by

$$|\delta \tan \phi| = (J^2 + \delta^2)^{1/2} - |J| \qquad (9)$$

and the distance of one inner line to a corresponding outer line is just the value of the exchange integral $|J|$.

The extension of the theory to include hyperfine interactions is straightforward.[26] The nuclear spin functions can be included in the basis set by using product functions of the form $|M_s, M_I^{(a)}, M_I^{(b)}\rangle$. Because in the high-field approximation the nuclear components of the spin states are not mixed by the Hamiltonian (1), eq 3, after the nuclear Zeeman terms are added, and (6)–(8) remain valid. Only the expressions (4) and (5) for ϵ and δ have to be modified resulting in different values for all possible combinations of the nuclear spin states. If only one magnetic nucleus is considered in each moiety, one obtains

$$\epsilon(M_I^{(a)},M_I^{(b)}) = {}^1/_2\beta B(g^{(a)} + g^{b})/h + {}^1/_2a^{(a)}M_I^{(a)} + {}^1/_2a^{(b)}M_I^{(b)} \qquad (10)$$

$$\delta(M_I^{(a)},M_I^{(b)}) = \beta B(g^{(a)} - g^{(b)})/h + a^{(a)}M_I^{(a)} - a^{(b)}M_I^{(b)} \qquad (11)$$

Hence two pairs of ESR lines (as described above) may show up for each combination of nuclear spin states ($M_I^{(a)}$, $M_I^{(b)}$, giving a maximum number of $4n_an_b$ lines, where n_a and n_b denote the numbers of hyperfine components present in the monoradical moieties. The splittings are determined by J and δ, and the relative intensities are given by pD_aD_b, where p is defined by eq 8 and D_a and D_b denote the degeneracies of the nuclear spin states.

In order to account for the ENDOR spectra, in eq 3 the nuclear Zeeman terms $(-\beta_n g_n^{(a)} BM_I^{(a)} - \beta_n g_n^{(b)} BM_I^{(b)})/h$ have to be included. First, the limiting cases shall be discussed. If the exchange interaction is large ($|J| \gg |a|, |\Delta g\beta B/h|$), ESR transitions to the state $|0-\rangle \equiv |0e\rangle$ are forbidden, and therefore the singlet level need not be considered. Moreover, the ESR transitions $|0+\rangle \leftrightarrow |1\rangle$ and $|-1\rangle \leftrightarrow |0+\rangle$ ($|0+\rangle \equiv |0_a\rangle$) are degenerate and the ENDOR resonance condition is given by[27]

$$\nu_k^{ENDOR} = |\nu_n - M_S a_k^t| \qquad (12)$$

where $\nu_n = \beta_n g_n B/h$, $M_S = -1$, 0, 1, and $a_k^t = a_k/2$ (vide supra).

On the other hand, in the limit of negligibly small exchange interaction, separate ENDOR spectra will be observed for the two monoradical moieties.

$$\nu_i^{ENDOR} = |\nu_n - m_S^{(a)} a_i^{(a)}|; \qquad m_S^{(a)} = \pm 1/2$$

$$\nu_j^{ENDOR} = |\nu_n - m_S^{(b)} a_j^{(b)}|; \qquad m_S^{(b)} = \pm 1/2 \qquad (13)$$

It is noteworthy that the ENDOR line positions (apart from the free nuclear frequency line; vide infra) are independent of the value of J, provided that the overlap between the molecular orbitals $|a\rangle$ and $|b\rangle$ can be neglected. However, in the case $J \simeq 0$, it depends on the ESR transition selected whether an ENDOR spectrum of fragment a (ESR transitions $\Delta m_S^{(a)} = \pm 1$, $\Delta m_S^{(b)} = 0$) or fragment b (ESR transitions $\Delta m_S^{(b)} = \pm 1$, $\Delta m_S^{(a)} = 0$) is observed.

The intermediate case $|J| \simeq |a|$ can qualitatively be understood in terms of the limiting cases if it is taken into account that the degeneracy of the ESR transitions is lifted. As a consequence, either the electron spin state $|1\rangle$ or the state $|-1\rangle$ will be involved in the ESR transition that is selectively pumped, and according to eq 12, only one ENDOR line is observable for each set of equivalent nuclei (the free nuclear frequency line will be discussed below). The position of this ENDOR line, either at $\nu_k^+ = \nu_n + |a_k^t|$ or at $\nu_k^- = |\nu_n - |a_k^t||$ depends upon the relative signs of J and a_k^t. The sign of the product $M_S a^t$ is directly given by the ENDOR line position; see (12). The sign of the product $M_S J$ can be deduced from the position of the ESR component being saturated. If the four ESR positions associated with an arbitrary combination of nuclear spin states are considered, the sequence given in eq 8 is in the order of decreasing energy (i.e., the resonance field strengths at constant microwave frequency are increasing) if J is positive and vice versa (sign ($\delta \tan \phi$) = sign J; see eq 6).

For biradicals with $|J| \gg |a|$, ENDOR lines at the free nuclear frequencies were predicted to arise from NMR transitions within the $M_S = 0$ electron spin state.[12] However, since the ESR transitions $|0_a\rangle \leftrightarrow |1\rangle$ and $|-1\rangle \leftrightarrow |0_a\rangle$ are degenerate, they are pumped equally strongly, thus leaving the thermal nuclear spin polarization in the $M_S = 0$ manifold undisturbed, and the free nuclear frequency line cannot be observed in liquid solution.[13] For the case in which J is still large but not much larger than a, it was calculated that this line should be split into a doublet (or a multiplet) separated by $a^2/2J$ if only one set of equivalent nuclei is present. The situation becomes even more complex if the biradical contains different types of nuclei. However, it can be estimated that in the case $|J| > |\delta| > |a_i|$ the splitting should be of the order of $a_i\delta/J$. Thus it is conceivable that the degeneracy of the ESR transitions is lifted due to the g-factor difference or some large hyperfine coupling, whereas the expression $a_i\delta/J$ might be smaller than the ENDOR line width for a *different* set of nuclei exhibiting much smaller coupling constants a_i and the free nuclear frequency line might become observable.

Results and Discussion

ENDOR of Monoradicals. For a proper understanding of the biradical spectra the knowledge of the g values and the hyperfine coupling constants of the constituent doublet-state species, i.e., galvinoxyls and nitroxides, is necessary. The appropriate model compound for all galvinoxyl moieties (except for those in **9b** and **13b**) is phenylgalvinoxyl (**1b**). The ENDOR spectrum of **1b** is depicted in Figure 2 (top), and the coupling constants are collected in Table II. The largest splittings are due to the phenoxy ring protons, which are slightly inequivalent at low temperatures. Whereas galvinoxyl radicals have been thoroughly investigated by ENDOR and TRIPLE resonance techniques.[27,29] only a few ENDOR studies of nitroxide radicals have been reported so

(29) Mukai, K.; Kamata, T.; Tamaki, T.; Ishizu, K. *Bull. Chem. Soc. Jpn.* **1976**, *49*, 3376. Hinrichs, K.; Kirste, B.; Kurreck, H.; Reusch, J. *Tetrahedron* **1977**, *33*, 151. Kirste, B.; Kurreck, H.; Schubert, K. *Ibid.* **1980**, *36*, 1985.

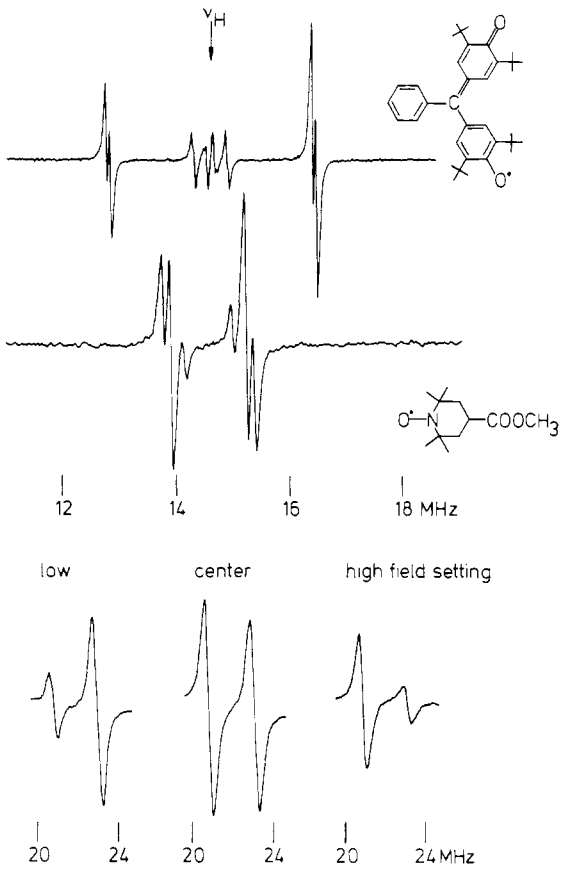

Figure 2. Top, ^{1}H ENDOR spectrum of phenylgalvinoxyl (**1b**, toluene, 195 K); center, ^{1}H ENDOR spectrum of **8** (toluene, 185 K); bottom, ^{14}N ENDOR spectra of **8** taken at different field settings (256 K, B_{NMR} = 0.71 mT (21 MHz) and 0.61 mT (23 MHz) in the rotating frame). Note that the ^{14}N ENDOR lines are centered around $a^N/2$ = 21.84 MHz, separations 2.190 ● 0.01, 2.285, and 2.215 MHz at B = 341.55, 343.11, and 344.68 mT, respectively; see text.

far.[30-32] Therefore, we have performed ^{1}H and ^{14}N ENDOR and TRIPLE experiments on a series of nitroxide monoradicals; see Figure 2 and Table II. Note that the ^{1}H ENDOR lines are centered around the free proton frequency ν_H ($|a|/2 < \nu_H$) whereas the ^{14}N ENDOR lines are centered around $a^N/2$ and separated by $2\nu_N$, neglecting second-order effects; vide infra ($|a|/2 > \nu_N$).

The proton hyperfine coupling constants, especially those of tanol (**7**), are markedly temperature dependent. This is evident from well-resolved ESR spectra and has been investigated by means of NMR;[33] yet well-resolved ^{1}H ENDOR spectra could only be obtained in a small temperature range. The ^{14}N hyperfine coupling constants are also temperature dependent (see Table II), and it is noteworthy that the temperature coefficients of the piperidinyloxyls like tanol (**7**) are negative, whereas those of tanone (**6**) and the pyrrolinyloxyls (e.g., **12**) are positive.

The general TRIPLE experiments[34] allowed the determination of the signs of the proton couplings relative to each other and also relative to that of the ^{14}N coupling; see Table II. The absolute sign of the isotropic ^{14}N coupling constant was assumed to be positive. This can be inferred from the ^{14}N hyperfine tensor data,[32,35] given the fact that the spin population at the nitrogen atom must be positive ($\rho^N \simeq 0.5$).[36] Consequently, the proton couplings should be negative, which is in agreement with the absolute signs deduced from ^{1}H NMR measurements on **6**[37] and **7**.[33]

It is evident from Figure 2 (bottom) that the relative amplitudes of the ^{14}N ENDOR lines depend markedly on the field setting, i.e., the M_I (^{14}N)-component in the ESR spectrum being saturated. This is indicative of cross-relaxation effects and the fact that the high- (low) frequency ENDOR line is more intense than the other, while irradiating the low- (high) field ESR component proves that the W_{x2} (flop–flop) process is dominant as compared to the W_{x1} (flip–flop) process[30]. (Cross-relaxation effects do not influence the relative ENDOR amplitudes for the center field setting.) The ratio R (≥ 1) of the high- and low-frequency ENDOR amplitudes (corrected for the hyperfine enhancement factor[38]) was found to be strongly temperature dependent; e.g., in the case of tanol (**7**; solvent toluene); R = 1.4 ± 0.1 (205 K), 2.9 (246 K), and 3.7 (288 K). The amplitude ratio depends upon the various relaxation rates (W_e, W_n, W_{x1}, W_{x2}, and ω_{HE}, the Heisenberg exchange rate), and it has been shown that R can be expressed as a function of three parameters[39]. Two of these parameters can be calculated from the various magnetic interactions (and ω_{HE}) and are independent of temperature, whereas the third parameter is the rotational correlation time, τ_c, which can be estimated from the Stokes–Einstein relation

$$\tau_c = {}^4/_3\pi r^3\eta/kT \qquad (14)$$

where r is an effective radius and η the viscosity of the solvent. A detailed discussion of these effects is beyond the scope of this study, yet it is noteworthy that an amplitude ratio of R = 1.5 ± 0.1 (288 K, toluene) was measured for the larger molecule **16a**. Since the magnetic parameters, i.e., the **g** and $\mathbf{A}^N$ tensors, are roughly equal in all nitroxides investigated here, this low value of R reflects an increase of the rotational correlation time τ_c caused by the larger molecule volume; see eq 14. For the same reason temperatures higher than in the case of the smaller molecules (**6–8**, **12**) were necessary to obtain a maximum ENDOR response.

Finally, some remarks concerning the second-order shifts shall be made. Correct to second order, the ENDOR frequencies for a nucleus with I = 1 are given by[40]

$M_I = -1$:

$$\nu^+ = |a/2 + \nu_N + 2s|$$
$$\nu^- = |a/2 - \nu_N| \qquad (15)$$

$M_I = +1$:

$$\nu^+ = |a/2 + \nu_N|$$
$$\nu^- = |a/2 - \nu_N - 2s| \qquad (16)$$

where $s = \langle a^2\rangle/4\nu_e$; all four transitions occur when the $M_I = 0$ hyperfine component is saturated. Consequently, the resonance lines are centered exactly around $|a/2|$ only for the center field setting ($M_I = 0$), and the line separations are given by $2\nu_N + 2s$ ($M_I = \pm 1$) or $2\nu_N + 4s$ ($M_I = 0$). In general, the second-order shifts may contain a contribution from the mean-square fluctuation terms $\langle(\delta a)^2\rangle$ in the hyperfine splitting, $\langle a^2\rangle = a^2 + \langle(\delta a)^2\rangle$.[40] This dynamic contribution was claimed to be of the same order of magnitude as the static part a^2 in the case of nitroxides.[30] However, in a series of careful measurements involving different nitroxide radicals at various temperatures we did *not* find such

(30) Leniart, D. S.; Vedrine, J. C.; Hyde, J. S. *Chem. Phys. Lett.* **1970**, *6*, 637.
(31) Dinse, K. P.; Möbius, K.; Plato, M.; Biehl, R.; Haustein, H. *Chem. Phys. Lett.* **1972**, *14*, 196. Atherton, N. M.; Brustolon, M. *Mol. Phys.* **1976**, *32*, 23.
(32) Percival, P. W.; Hyde, J. S.; Dalton, L. A.; Dalton, L. R. *J. Chem. Phys.* **1975**, *62*, 4332.
(33) Brière, R.; Lemaire, H.; Rassat, A.; Dunand, J.-J. *Bull. Soc. Chim. Fr.* **1970**, 4220.
(34) Möbius, K.; Biehl, R. In "Multiple Electron Resonance Spectroscopy"; Dorio, M. M., Freed, J. H., Eds.; Plenum Press: New York, 1979; p 475.
(35) Polnaszek, C. F.; Freed, J. H. *J. Phys. Chem.* **1975**, *79*, 2283. Smith, W.; Kispert, L. D. *J. Chem. Soc., Faraday Trans. 2* **1977**, *73*, 152.
(36) Aurich, H. G.; Hahn, K.; Stork, K.; Weiss, W. *Tetrahedron* **1977**, *33*, 969.
(37) Kreilick, R. W. *J. Chem. Phys.* **1967**, *46*, 4260.
(38) Geschwind, S. In "Hyperfine Interactions"; Freeman, A. J., Frankel, R. B., Eds.; Academic Press: New York, 1967.
(39) Fey, H.-J.; Lubitz, W.; Zimmermann, H.; Plato, M.; Möbius, K.; Biehl, R. *Z. Naturforsch, A* **1978**, *33A*, 514.
(40) Atherton, N. M. In "Multiple Electron Resonance Spectroscopy"; Dorio, M. M., Freed, J. H., Eds.; Plenum Press: New York, 1979; p 143.

Table III. g Values, Hyperfine Coupling Constants (MHz), Exchange Integrals (MHz), and Zero-Field Splitting Parameters (MHz) of Biradicals[a]

	g[b]	a^H(phenoxy)	a^H(nitroxide)	a^N	J	$\|D\|$
9b				(+)43.1[c]	$\gg a^N$	200
10b	2.00542	+3.68	−1.33	+43.38	−145	58
11b		+3.66	−1.35	+43.57	−25.0	$< a^N$[d]
13b				+40.8[c]	$\gg a^N$	196
14b	≃2.0054			+39.8[c]	$\gg a^N$	163
15b	2.00529				|163|	85
16b	2.00530	+3.60	−0.64	+39.73	−167	58
17b	2.00531				|32|	$< a^N$[d]

[a] Solvent toluene; g, a^N, and J values were measured at 290 K, a^H was measured at 225 K, and D parameters were measured at 160 K. The HFSC's are given as "doublet" constants; cf. text, eq 1; measured by ENDOR, accurate within ±0.02 (a^H) and 0.1 MHz (a^N). [b] Accurate measurements of the g values of **9b**, **11b**, and **13b** were prevented by large line widths and/or superimposed signals from monoradical impurities. [c] Measured by ESR, ±0.3 MHz. Note that the line spacing is given by $a^t = a^N/2$. [d] Zero-field splitting smaller than ^{14}N hyperfine anisotropy.

a contribution within experimental error (see Figure 2, caption; ν_N = 1.055 MHz at 343 mT, s = (0.045 ± 0.005) MHz, calculated 0.050 MHz from the static part only).

ESR of Biradicals. Figure 3a shows the ESR spectrum of the mixed biradical **14b** (290 K), consisting essentially of three broad lines separated by 0.71 mT. This is half the value of the respective nitroxide monoradical. Moreover, the g value is just the average of the galvinoxyl and nitroxide g values; see Tables II and III. Consequently, the exchange interaction in biradical **14b** must be much larger than the hyperfine interaction ($|J| \gg |a|$), and the ^{14}N hyperfine splitting is given by $a^t = a^N/2$ = 19.9 MHz. The additional features superimposed on the biradical spectrum become more pronounced on lowering the temperature when the biradical lines are broadened out; see Figure 3b. We assign them to galvinoxyl and nitroxide monoradical impurities present in the sample (vide infra). For comparison, the ESR spectra of the monoradicals **1b** and **14a** are also included in Figure 3c,d. The relatively large widths of the biradical lines, especially at lower temperatures, are caused by the zero-field splitting. In fact, a spectrum showing the characteristic features of a powder spectrum of randomly oriented triplets with superimposed ^{14}N hyperfine structure could be observed in glassy toluene (160 K), yielding a D parameter of 163 MHz.[41] It should be noted that a spectrum similar to that assigned to the mixture of monoradicals (requiring the proper intensity ratio) might, in principle, arise from another conformation of the biradical with $|J| \ll |a|$ and negligibly small zero-field splitting. However, in view of the results obtained for the other biradicals, we exclude this possibility. We wish to point out that small amounts of monoradical impurities, accounting for a few percent of the total paramagnetic resonance absorption, were inevitably present in the solutions of all biradicals studied here. Since the galvinol/nitroxide precursors are chemically pure (elemental analyses, thin-layer chromatography), we assume that these impurities arise from decomposition of one of the constituent radical moieties during or after the final oxidation step. Similar phenomena are well-known from investigations of bis(galvinoxyls)[5] and other biradicals. Since the monoradical resonances are easily identified (cf. Table II) and since the temperature dependence of their positions and line shapes is small (see Figure 3), their presence does not interfere with the biradical spectra.

The ESR spectra of three galvinoxyl/nitroxide biradicals with connecting bridges of different lengths are shown in Figure 4 (left). The spectrum of biradical **9b** (Figure 4, top) is analogous to that of **14b**, discussed in the previous paragraph; i.e., $|J| \gg |a|$, ^{14}N hyperfine splitting $a^t = a^N/2$ = 21.6 MHz, and a substantial line broadening shows up, caused by the modulation of the zero-field splitting. The spectrum of biradical **10b** (Figure 4, center), however, exhibits additional splittings and is not symmetric about its center. It consists of five components; two of them (b and d) show a quintet pattern (line spacings ≃ 0.089 mT). Clearly, the condition $|J| \gg |a^N|$ is not fulfilled for biradical **10b**, but the spectrum can readily be analyzed by means of the calculated stick spectra given in Figure 5 for different values of J relative to a^N.

(41) Krüger, A. Thesis (unpublished results), FU Berlin, 1981.

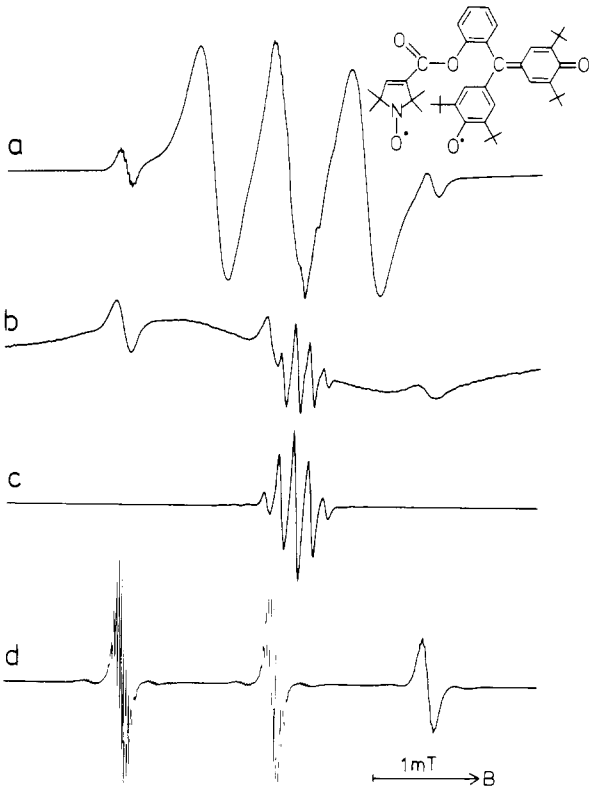

Figure 3. ESR spectra of a solution of biradical **14b** in toluene at 290 K (a) and 215 K (b); see text. For comparison, the ESR spectra of the monoradicals **1b** (c) and **14a** (d) are also shown (toluene, 290 K).

Obviously $|J| > |a^N|$ for biradical **10b** is valid, and the value of the exchange integral can be calculated by using eq 9 and 11 and the g values and hyperfine coupling constants from the constituent monoradical moieties (Table II). For example, the separation of the ESR components a and b is found to be 0.307 mT (8.62 MHz), and with a calculated value of δ = 50.8 MHz (i.e., the sum of a^N and $\Delta g\beta B/h$), $|J|$ = 145 MHz is obtained. The quintet pattern of the ESR components b and d arising from the proton hyperfine interaction within the galvinoxyl moiety (not included in Figure 5) is well reproduced in a computer-simulated spectrum (Figure 4, right). A comparison of the ESR spectrum of biradical **11b** (Figure 4, bottom) with the stick spectra given in Figure 5 reveals that $|J| < |a^N|$ in this case. Consequently, the exchange integral is directly obtained from the separation of the components a and b or h and i, yielding $|J|$ = 25 MHz. In fact, the spectrum can be visualized as a superposition of a "nitroxide" and a "galvinoxyl" spectrum, both of them exhibiting additional splittings due to the exchange interaction.

Whereas the ESR spectra of biradical **16b** are similar to those of the related biradical **10b**, the appearance of the spectra of

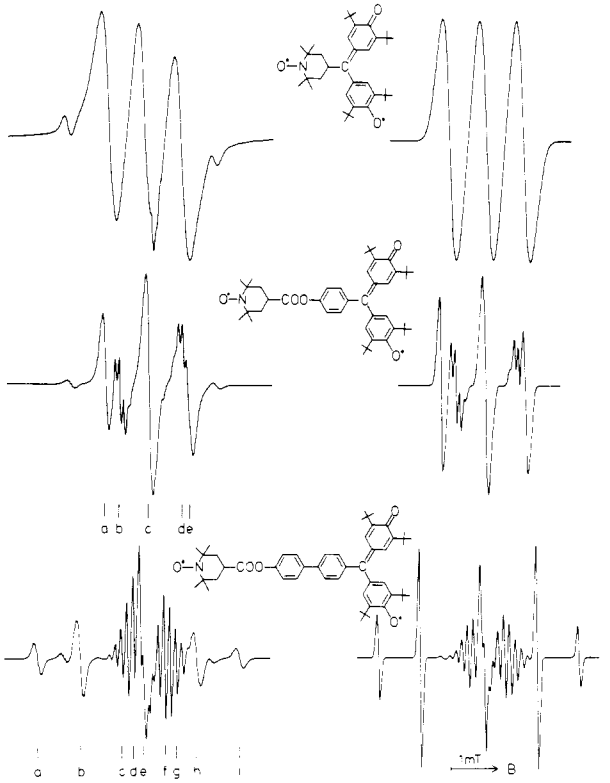

Figure 4. ESR spectra (left; toluene, 290 K) and computer-simulated spectra (right) of biradicals **9b** (top), **10b** (center), and **11b** (bottom). The line widths do not match for all lines since the proton HFS of the nitroxide moiety and the M_I dependence have not been taken into account in the simulations. The marked field positions refer to the ENDOR measurements; see text and Figures 7–9.

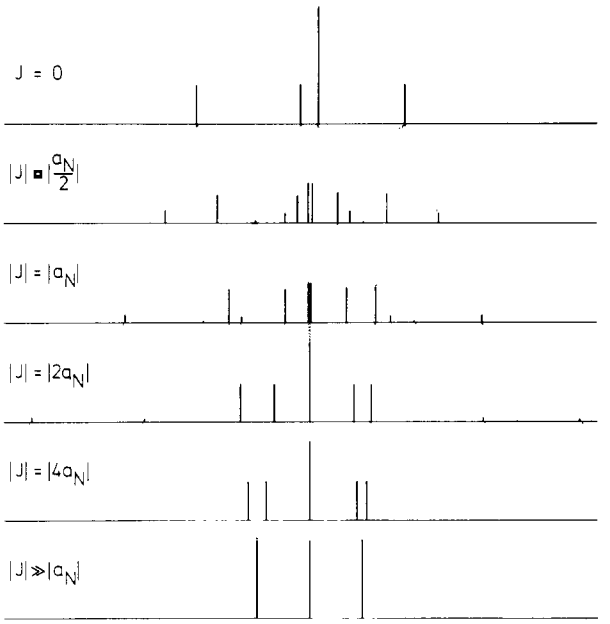

Figure 5. Calculated line positions and intensities for a mixed galvinoxyl/nitroxide biradical for various relative values of J and a^N. For simplification, the proton HFS has been omitted. Note that the spectra are unsymmetrical unless $|J| \gg |a^N|$ because of the different g values of the monoradical moieties.

biradical **17b** is strikingly different from those of **11b**; see Figure 6. The outer lines in the spectrum taken at 310 K (Figure 6, top) are much broader and correspondingly smaller than the others. Moreover, when the temperature is lowered, the positions of these lines are shifted toward the center of the spectrum; i.e., the value of the exchange integral J is decreasing. However, it

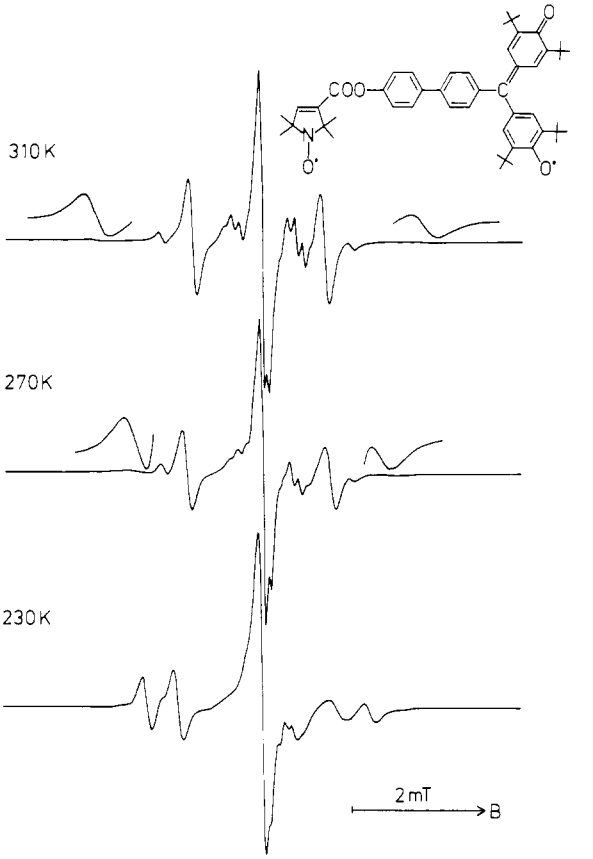

Figure 6. ESR spectra of biradical **17b** at different temperatures (solvent toluene). The insets in the spectra taken at 310 and 270 K show the wings at a higher gain (× 20).

is not possible to describe (or simulate) the spectra taken at the lower temperatures by means of a single value of J. Instead, a careful inspection of the spectrum taken at 230 K reveals that it is a superposition of the spectra of different species, i.e., different conformations of the biradical. The line-broadening effects can be explained by assuming that these conformations are interconverting, with a rate constant within the ESR time scale. Similar dynamic processes giving rise to a modulation of J have been observed for other biradicals.[42] Whereas the absolute value of the exchange integral J is decreasing on lowering the temperature in the case of **17b** (from 41 MHz at 310 K to about 10 MHz at 210 K, regarding the dominant conformations), an increase is found for biradical **11b** (from 24.0 MHz at 310 K to 31.0 MHz at 210 K).

ENDOR of Biradicals. Figure 7 shows the ^1H and ^{14}N ENDOR spectra of biradical **11b** obtained with the center field setting, i.e., the ESR component $M_I(^{14}N) = 0$. The two pairs of lines showing up in the ^1H ENDOR spectrum can be assigned to the galvinoxyl ring protons and the methyl protons within the nitroxide moiety. By comparison with Figure 2 it is evident that the line positions are the same as in the respective monoradical spectra, whereas the line widths are substantially larger. Thus the resolution is decreased and ENDOR lines from small couplings cannot be observed. Such a behavior was also found in previous fluid solution ENDOR studies of symmetric biradicals[13,43] and can be attributed to an additional contribution to the electron spin–lattice relaxation rate W_e caused by the electron–electron dipolar interaction. The fact that the coupling constants of the biradical can be directly taken from the ENDOR spectrum is quite remarkable since the line separations in the ESR spectrum of a biradical with $|J| \simeq |a|$ do not represent the hyperfine splittings; see Figure 4 and the

(42) Luckhurst, G. R. *Mol. Phys.* **1966**, *10*, 543. Lemaire, H.; Rassat, A.; Rey, P. *Bull. Soc. Chim. Fr.* **1968**, 886. Giroud, A. M.; Rassat, A. *Ibid.* **1979**, 48.

(43) Kirste, B.; Kurreck, H.; Schubert, K. *Tetrahedron Lett.* **1978**, 777.

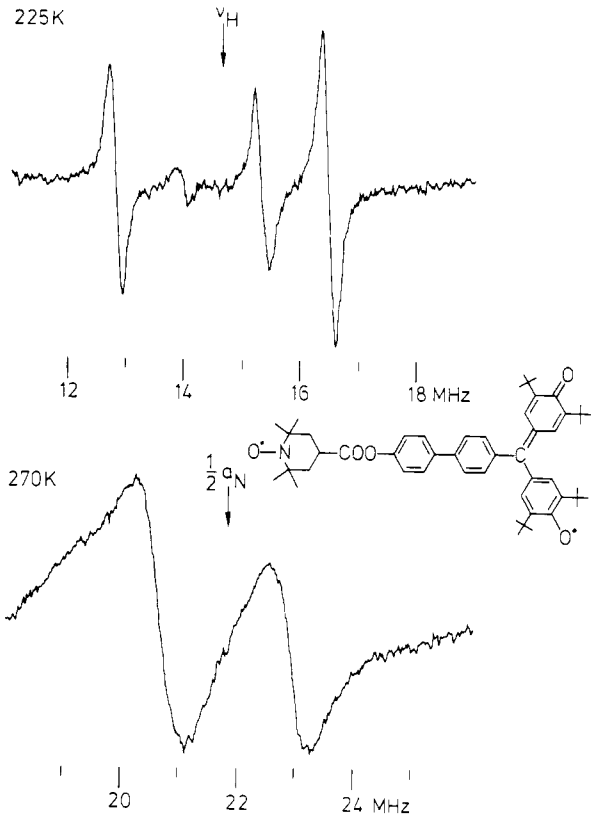

Figure 7. ^1H (top) and ^{14}N (bottom) ENDOR spectra of biradical **11b** at the center field setting (position e in Figure 4, bottom). Solvent toluene, $B_{NMR} \simeq 0.5$ mT (^1H) and 0.76–0.66 mT (^{14}N) in the rotating frame, microwave power 80 mW.

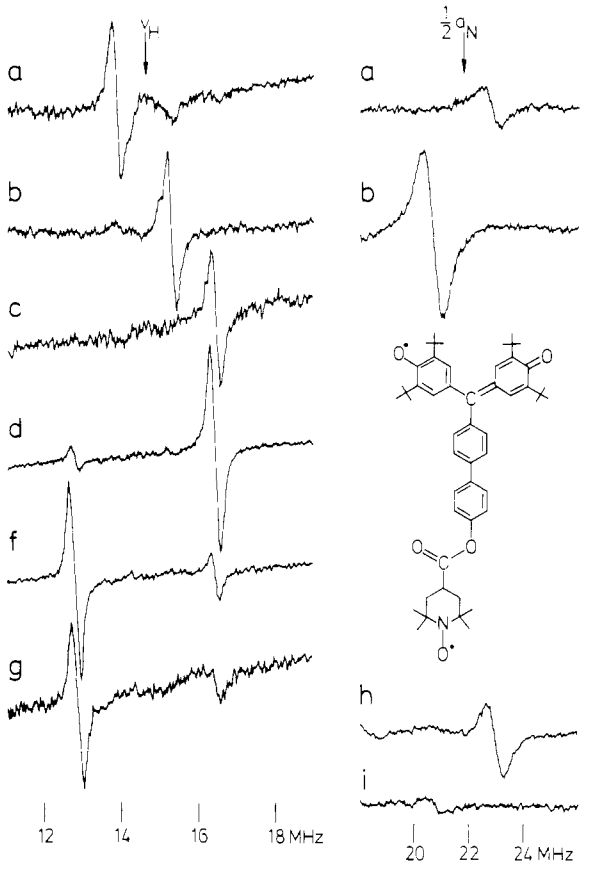

Figure 8. ^1H (left) and ^{14}N (right) ENDOR spectra of biradical **11b** at different off-center field settings (cf. Figure 4, bottom). The experimental conditions are comparable to those given in Figure 7.

discussion presented above. It should be noted that the condition $|J| \gg |\delta|$ is fulfilled for the central ESR component (see eq 11). Therefore only the two ESR transitions within the "triplet" manifold are allowed and approximately degenerate (see eq 8). Hence, ENDOR lines arising from NMR transitions in both the $M_S = +1$ and $M_S = -1$ manifolds can be observed.

The situation becomes quite different when ENDOR spectra taken at various off-center field settings are considered; see Figure 8. Depending upon the ESR component being saturated, ^1H and ^{14}N ENDOR lines either from the galvinoxyl or from the nitroxide moiety show up. Moreover, only one ENDOR line from each coupling can be observed (or is at least much more intense than the other). The former effect can be rationalized as follows. The exchange integral is relatively small ($|J| = 25$ MHz) and the condition $|J| < |\delta|$ is fulfilled for the ESR components $M_I(^{14}N) = \pm 1$. Therefore the ESR components of the biradical can be classified as "nitroxide" (components a, b, h, *i* see Figure 4, bottom) or "galvinoxyl" lines (components c, d, f, g), which manifests itself in the proton hyperfine structure. Thus, only the respective ENDOR lines can be observed since NMR transitions associated with the other moiety cannot open an effective relaxation pathway. The fact that either the high- or low-frequency ENDOR line shows up is caused by the exchange interaction and not by cross-relaxation effects. It can be understood by considering the influence of the exchange interaction on the energy levels of a biradical, eq 3. Whereas the levels $M_S = 1$ and $M_S = -1$ are merely shifted, thus leaving the NMR transitions within these manifolds undisturbed, there is a mixing of the $M_S = 0$ triplet sublevel with the singlet level. It has been shown theoretically that this mixing should strongly affect the respective NMR transitions, resulting in a complex pattern of the ENDOR lines if the exchange integral is roughly equal in magnitude to the hyperfine coupling constants.[12] Obviously, such lines are not present in the ENDOR spectra obtained for biradical **11b** (see Figure 8), and the observed signals must be due to NMR transitions within either the $M_S = 1$ or the $M_S = -1$ manifolds. The important point to note is that only one of these levels is involved in each ESR transition associated with any off-center component. It is now straightforward to deduce the relative signs of the exchange integral J and the hyperfine coupling constants. For example, only the high-frequency ^{14}N ENDOR line is observed at position a (see Figures 8 and 4). If a^N is taken to be positive, according to the resonance condition, eq 12, this line must arise from the $M_S = -1$ manifold. The ESR component a is the ultimate low-field component, arising from the transition $|0-\rangle \leftrightarrow |1\rangle$ if $J > 0$ or from the transition $|1-\rangle \leftrightarrow |0-\rangle$ if $J < 0$; see eq 8. Now it is evident from the ENDOR experiment that J is *negative* since the level $M_S = -1$ must be involved. This means that the triplet state is the ground state. A further analysis yields a negative sign for the methyl proton coupling of the nitroxide moiety and a positive sign for the galvinoxyl ring proton coupling. These results, consistently obtained for the different field settings, are in agreement with the TRIPLE experiments performed on the monoradicals (vide supra).

The ENDOR spectrum of biradical **10b** obtained for the center field setting is similar to that depicted in Figure 7; the coupling constants are collected in Table III. The ^1H and ^{14}N ENDOR spectra taken at different off-center field settings are shown in Figure 9. Both "galvinoxyl" and "nitroxide" lines show up at any field setting, with either the high- or low- frequency line being much more intense (the appearance of the weaker lines is due to the overlap of the ESR components; see Figure 4). Again it is possible to derive the relative signs of J and a_i. Since $|J| > |a|$ in this case, only transitions within the "triplet" manifold contribute to the ESR spectrum. thus, the low-field component a arises from the transition $|-1\rangle \leftrightarrow |0+\rangle$ if $J > 0$ or $|0+\rangle \leftrightarrow |1\rangle$ if $J < 0$. Since this field setting gives rise to the low-frequency ^{14}N ENDOR line ($M_S = 1$), J must be negative. The signs of the proton couplings deduced from the respective ^1H ENDOR spectrum are in accordance with those of **11b**; see Table III.

It is noteworthy that the fluid solution ENDOR spectra of biradical **10b** show a line at the free proton frequency that is most

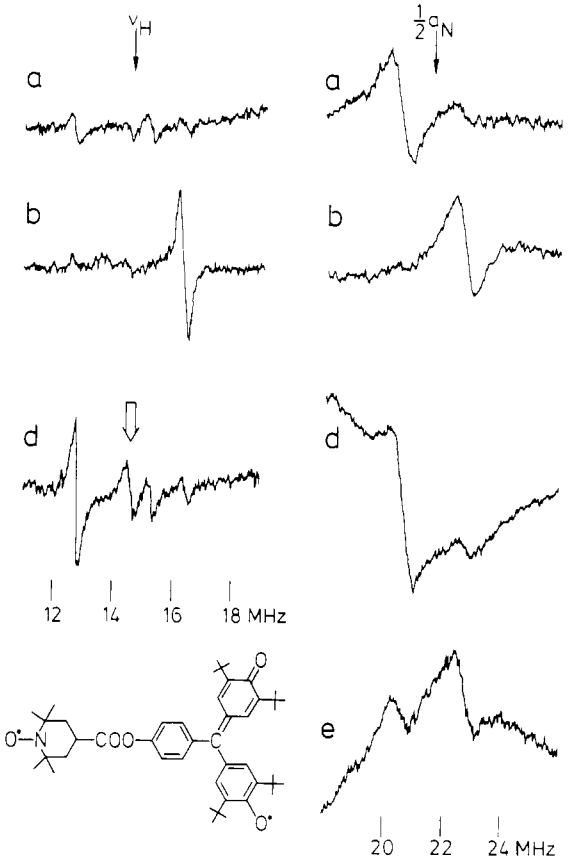

Figure 9. ^1H (left) and ^{14}N (right) ENDOR spectra of biradical **10b** at different off-center field settings (cf. Figure 4, center). Note the appearance of an ENDOR line at the free proton frequency (see arrow in spectrum d, left).

intense for the field setting d; see Figure 9. According to the arguments presented in the Theory, this "free proton frequency line" presumably arises from NMR transitions of protons with small coupling constants, e.g., *tert*-butyl protons, within the $M_S = 0$ manifold.

Finally, it should be mentioned that ENDOR spectra could also be obtained from biradical **16b**. The results are analogous to those for **10b**; see Table III. Attempts to record fluid solution ENDOR spectra of biradicals with larger zero-field splittings, e.g., **9b**, however, failed because of the strong relaxation processes caused by the electron–electron dipolar interaction. Thus it can be stated that under the experimental conditions used in this investigation (e.g., magnitude of microwave and radiofrequency power), successful fluid solution ENDOR on biradicals can only be performed for D values $< \sim 100$ MHz.

Conclusions

It has been shown that mixed galvinoxyl/nitroxide biradicals are suitable model compounds for the study of electron–electron spin exchange between different types of radicals. The magnitude of the exchange integral J relative to that of the nitrogen hyperfine coupling constant a^N varies from $|J| < |a^N|$ to $|J| \gg |a^N|$, depending on the length of the connecting bridge. Whereas the splittings observed in the ESR spectra do not represent the hyperfine coupling constants when the exchange integral has about the same magnitude, the ENDOR technique allows *direct measurements* of these coupling constants. Moreover, by means of ENDOR experiments it is possible to deduce the *sign of the exchange integral* relative to those of the hyperfine couplings. This is remarkable, since the sign determination from ESR is restricted to favorable cases and requires an elaborate analysis[15,16] and susceptibility measurements are not applicable if the exchange integral is small (i.e., $|J| \ll kT$). Actually, in the present paper the signs of the exchange integral could be determined for three of the mixed galvinoxyl/nitroxide biradicals and were found to be negative. Hence in these systems the triplet state unambiguously is the ground state. This is in contrast to several symmetrical bis(nitroxides) for which a positive sign of J was deduced.[15,16]

Finally, it should be pointed out that the present investigation opens an interesting aspect for the "absolute" sign determination of hyperfine coupling constants. It might be possible to prepare a weakly coupled biradical from the radical under study by means of the spin-labeling technique. An ENDOR experiment will then allow the determination of the signs relative to those of the spin label assumed to be known.

Acknowledgment. We are indebted to E. Brinkhaus, Freie Universität Berlin, for performing very careful ESR measurements. This work was supported by the Deutsche Forschungsgemeinschaft (Normalverfahren) and by the Fonds der Chemischen Industrie, which is gratefully acknowledged.

Registry No. 1b, 14635-89-3; **2a**, 81790-03-6; **3a**, 81769-81-5; **4a**, 81769-82-6; **5a**, 81769-83-7; **6**, 2896-70-0; **7**, 2226-96-2; **8**, 54416-73-8; **9a**, 81769-84-8; **9b**, 81790-04-7; **10a**, 81769-85-9; **10b**, 81769-86-0; **11a**, 81769-87-1; **11b**, 81769-88-2; **12**, 2154-32-7; **13a**, 81769-89-3; **13b**, 81769-90-6; **14a**, 81769-91-7; **14b**, 81769-92-8; **15a**, 81769-93-9; **15b**, 81769-94-0; **16a**, 81769-95-1; **16b**, 81769-96-2; **17a**, 81769-97-3; **17b**, 81769-98-4.

Perpendicular and Parallel Acetylene Complexes

David M. Hoffman, Roald Hoffmann,* and C. Richard Fisel

Contribution from the Department of Chemistry, Cornell University, Ithaca, New York 14853.
Received September 21, 1981

Abstract: A molecular orbital analysis of $L_3M(acetylene)ML_3$ complexes serves as an introduction to a general study of perpendicular- and parallel-bonded dinuclear transition-metal acetylene complexes. The two alternative geometries have different electronic requirements—the perpendicular acetylene has four frontier orbitals above a d^6–d^6 block and a metal–metal bond, the parallel-bonded acetylene has five such orbitals. Parallel and perpendicular acetylenes coexist for the same metal d-electron count, yet their interconversion by a simple twisting is not a likely process. If not forbidden by a level crossing, twisting generates instabilities that are relieved by a change in the coordination geometry of the metal. Isolobal analogies relating the acetylene complexes to tetrahedrane, olefins, and cyclobutadiene are a useful guide to their transformations.

As one examines dinuclear transition-metal complexes with bridging acetylene, $L_nM(acetylene)ML_n$, one is first struck by the structural diversity of the L_nMML_n moiety. Yet there is a clear partitioning, a dichotomy of all the known complexes; the acetylene is invariably situated nearly parallel, **1a**, or nearly perpendicular, **1b**, to the M–M vector. In Table I is given a partial listing, with

0002-7863/82/1504-3858$01.25/0